

Observation of Pure Spin Transport in a Diamond Spin Wire

J. Cardellino^{†,1}, N. Scozzaro^{†,1}, M. R. Herman¹, A. Berger¹, C. Zhang¹, K.C. Fong¹,
C. Jayaprakash¹, D.V. Pelekhov¹, P.C. Hammel^{1,*}

May 26, 2022

Spin transport electronics – spintronics – focuses on utilizing electron spin as a state variable for quantum and classical information processing and storage [1]. Some insulating materials, such as diamond, offer defect centers whose associated spins are well-isolated from their environment giving them long coherence times [2–4]; however, spin interactions are important for transport [5], entanglement [6], and read-out [7]. Here, we report direct measurement of pure spin transport – free of any charge motion – within a nanoscale quasi 1D ‘spin wire’, and find a spin diffusion length ~ 700 nm. We exploit the statistical fluctuations of a small number of spins [8] ($\sqrt{N} < 100$ net spins) which are in thermal equilibrium and have no imposed polarization gradient. The spin transport proceeds by means of magnetic dipole interactions that induce flip-flop transitions [9], a mechanism that can enable highly efficient, even reversible [10], pure spin currents. To further study the dynamics within the spin wire, we implement a magnetic resonance protocol that improves spatial resolution and provides nanoscale spectroscopic information which confirms the observed spin transport. This spectroscopic tool opens a potential route for spatially encoding spin information in long-lived nuclear spin states. Our measurements probe intrinsic spin dynamics at the nanometre scale, providing detailed insight needed for practical devices which seek to control spin.

Understanding and controlling spin transport is a central challenge in spintronics and has been extensively studied in systems where the spin density is large and treated as a continuum variable [11]. However, an understanding at the few spin level is needed for miniaturization and quantum applications. Appropriate and well-controlled coupling between spins can allow for efficient spin transport, while preserving long spin lifetimes. For example, two-spin flip-flop transitions – the simultaneous flipping of a pair of anti-aligned neighbouring spins due to their dipolar interaction – conserve magnetization, and successive flip-flops can result in a pure, diffusive spin transport [9, 12], as reported here. In contrast to non-equilibrium experiments [13, 14] which measure thermal polarization recovery, we monitor the spin noise [8, 15], which arises from statistical fluctuations. This allows us to observe the intrinsic thermal equilibrium spin dynamics of the ensemble [16].

In macroscopic systems containing a large number of particles, Fick’s law of diffusion describes the time evolution of particles moving from regions of high to low concentration, resulting in a smooth evolution toward equilibrium. By contrast, in few-spin ensembles fluctuations can lead to transient polarizations much larger than the Boltzmann (thermal) polarization, and even flow “against” the polarization gradient [17]. Our measurements focus not on the polarization itself, but on the time auto-correlation of the polarization in a nanoscale spin detection volume. In our experiments, these correlations are lost as a consequence of spin transport out of our measurement volume. We model this process using numerical simulations that incorporate this inherent randomness of few-spin, statistically-polarized ensembles, and our model corroborates our measurements.

In order to study flip-flop-dominated spin dynamics, we

[†] These authors contributed equally to this work

¹ Department of Physics, Ohio State University, Columbus, Ohio 43210, USA.

* Corresponding Author: hammel@physics.osu.edu

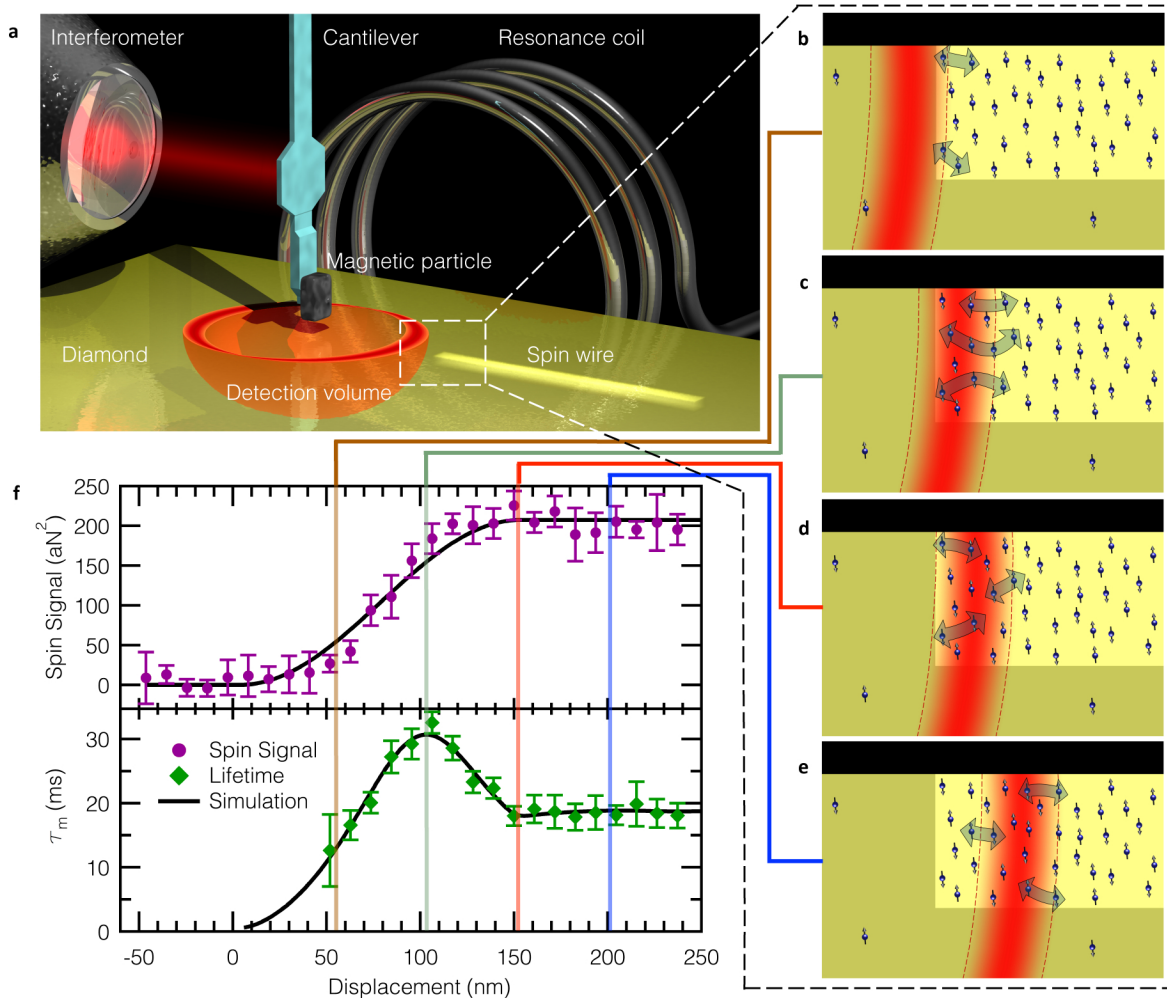


Figure 1: **MRFM spin wire setup, schematic of spin dynamics in wire, and spin noise measurements.** **a**, MRFM setup for measuring spin noise in the $200 \text{ nm} \times 250 \text{ nm} \times 4 \mu\text{m}$ spin wire of P1 centres in diamond. The coil excites resonance along a contour of the magnetic particle's field (plus an external field), called the 'resonant slice'. As the cantilever oscillates, the field due to the magnetic particle varies and the slice sweeps out the spin detection volume. Spins toward the centre of the detection volume contribute to the spin signal more strongly (solid red) than those near the edge. **b-e**, Schematic showing the detection volume as it is walked into the spin wire, the rectangular stripe region. The thick double arrows represent flip-flop-mediated spin diffusion in and out of the detection volume. **f**, The spin signal increases as a function of walk-in distance until the volume is fully inside the spin wire as in (e). **g**, The correlation time of the measured spins. At first (as in **b**) spins are able to quickly diffuse out of the volume, but as the measurement volume is walked in further (as in **c**), spins must diffuse a longer distance to exit the volume, causing the correlation time to increase. Once the measurement volume is fully inside the stripe (**d** and **e**), spins can diffuse out on both sides, decreasing the correlation time to roughly half the peak value.

fabricated a nanoscale channel of implanted nitrogen (P1) centres in diamond at a density of 6 ppm. At this density the strength of the dipolar coupling between spins is strong, leading to a flip-flop time, $T_{\text{ff}} \sim 10^{-4}$ s, several orders of magnitude shorter than $T_1 \sim 1$ s. The density outside the spin wire (0.3 ppm) is sufficiently small such that flip-flop transitions out of the wire are very rare, thus confining the spin transport to the wire.

We use magnetic resonance force microscopy (MRFM) to probe the spins within the wire (Fig. 1a). The force detector is an IBM-style ultra-soft cantilever [18] with a SmCo_5 magnetic particle glued onto the tip. To resonantly detect spins, we implement the iOSCAR timing protocol [8, 19]. A superconducting niobium coil is used to drive the spin resonance at a frequency of $\omega_{\text{rf}} = 2.18$ GHz. This frequency defines a ‘resonant slice’ where the total magnetic field (tip field plus external field) experienced by sample spins is equal to $\frac{\omega_{\text{rf}}}{\gamma} = 778$ G. By driving the cantilever at its self-determined resonant frequency to an amplitude of 150 nm, the resonant slice sweeps out a volume of this width, hereafter termed the detection volume.

We scan the detection volume into the spin wire (Fig. 1b-e) and measure the force exerted on the cantilever by the selected spins. From this measurement we can extract two quantities: spin signal (Fig. 1f, top), and the force correlation time τ_m (Fig. 1f, bottom). The spin signal is obtained from the variance in the time record of the force signal and is directly related to the number of measured spins [19]. τ_m describes the characteristic time for the net moment of the detected spins to decorrelate. This can be viewed as the time needed to transport spin out of the detection volume via a random-walk diffusion processes, with each step taking an average time T_{ff} . Once the detection volume enters the spin wire, the signal grows with the number of detected spins, eventually reaching a plateau when completely within the wire. The correlation time shows a complex behaviour as the detection volume moves into the wire. These results can be understood within the framework of flip-flop-mediated spin transport: ensemble correlation is lost as spins diffuse into or out of the detection volume. Just inside a displacement of 0 nm (Fig. 1b), the spins inside the volume easily and rapidly interact with nearby outside neighbours, resulting in a relatively short correlation time. With increasing overlap of the detection volume and the spin wire, spins must

diffuse further to exit the detection volume and change the overall magnetization of the ensemble, thus increasing τ_m . The correlation time peaks when approximately 68% of the detection volume has entered the spin wire (Fig. 1c). This is attributed to the force sensitivity profile of the detection volume: spins in the middle of the volume are most sensitively detected (solid red indicates highest sensitivity in Fig. 1), while the edges are least sensitive (see SI). As the detection volume approaches 100% overlap (Fig. 1d), spins are able to diffuse out either side of the most sensitive region, reducing the correlation time by roughly a factor of 2. Scanning deeper into the spin wire results in no further change, since the measurement geometry becomes translationally invariant (Fig. 1e).

A global measurement of the spin polarization, encompassing the entire spin wire, would not uncover this magnetization-preserving spin transport process. In the opposite limit of measuring a single spin, T_1 -type spin relaxation becomes indistinguishable from flip-flop induced polarization changes. By systematically varying the size of the overlap of the detection volume with the spin wire, and hence the number of detected spins, our measurement of τ_m reveals the observed signature of spin transport. This is similar to measurements of spin lifetime by electrically- or optically-detected Hanle signals [11, 20, 21], where diffusion of spins away from the detection volume (electrical contact or optical probe spot) can influence spin dephasing.

Since the average polarization gradient vanishes at thermal equilibrium, the conventional model of diffusion driven by polarization gradient predicts that τ_m will be independent of detection volume position within our thermal equilibrium wire. Such a model neglects the dominant role spin fluctuations play in nanoscale ensembles. In order to fit the measured data in Fig. 1f, we use a Monte Carlo simulation which models the flip-flops between individual spins as a Markov process (see SI). From this fit we can extract the flip-flop time, $T_{\text{ff}} = 0.21$ ms, and the corresponding diffusion constant of $D = \frac{a^2}{T_{\text{ff}}} = 4.6 \times 10^{-9} \frac{\text{cm}^2}{\text{s}}$, where $a = n^{-1/3} = 9.82$ nm is the average nearest-neighbour separation of spins with a density $n = 1.06 \times 10^{18} \text{ cm}^{-3}$ (6 ppm). We find good agreement comparing this to the theoretical flip-flop time [12] $T_{\text{ff,th}} = 30 T_2 = 0.36$ ms, where we have used $T_2 = 11.9 \mu\text{s}$, which arises from dipolar interactions (at a density of 6 ppm) and has been experimentally verified [22]. We

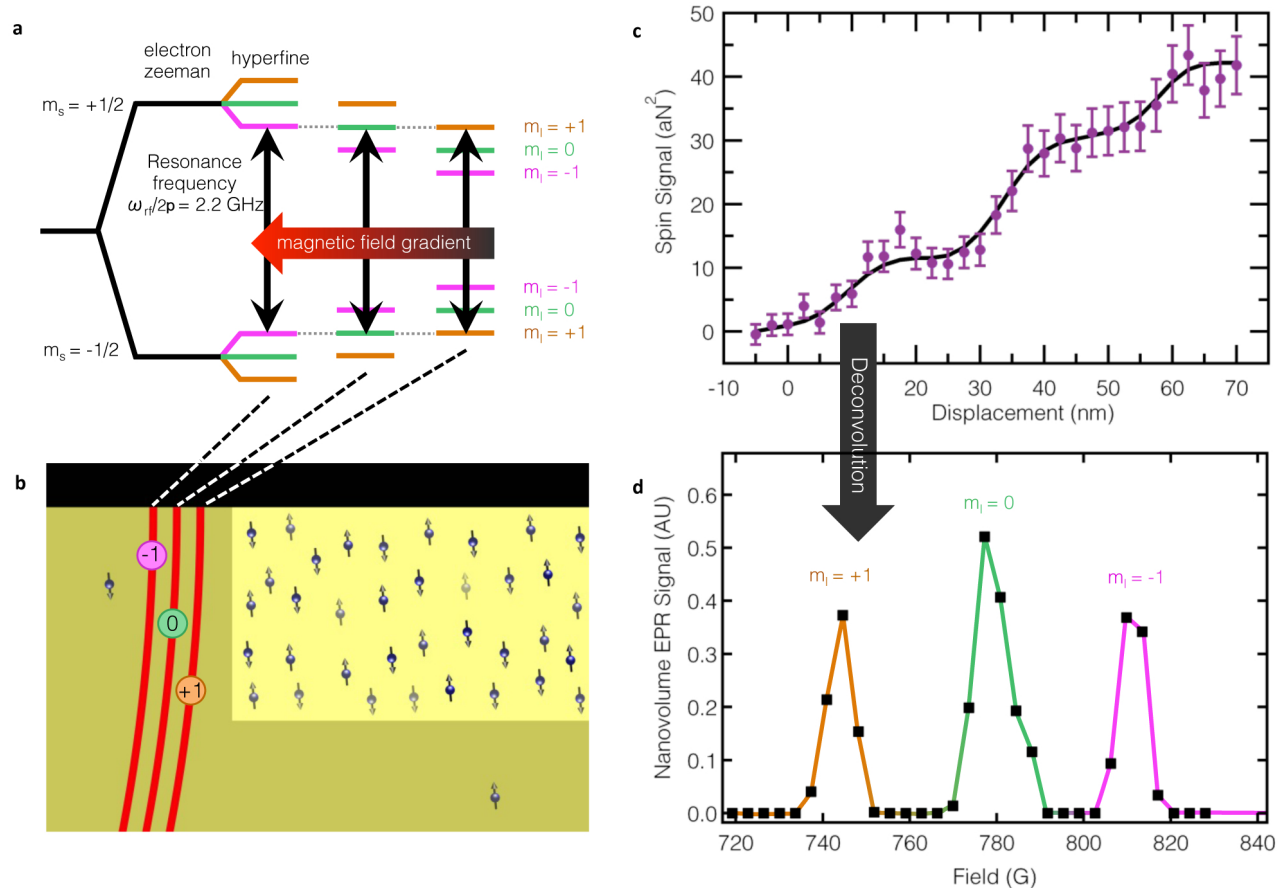


Figure 2: **Hyperfine spectrum measurement for spin wire.** **a**, Energy level diagrams for three hyperfine-split spin populations, which are simultaneously on resonance, yet spatially separated by the gradient. **b**, Schematic of the three volumes which are walked into the spin wire. **c**, The spin signal increases in a step-like fashion as each volume enters the wire. **d**, A nanovolume EPR spectrum can be obtained by deconvolving the spin signal with the known force sensitivity (see SI) and the three hyperfine peaks are resolved.

furthermore find a diffusion length $L = \sqrt{DT_1} = 720$ nm, which is significantly larger than the lateral dimensions of the wire (depth 250 nm, width 200 nm, and length 4 μm). This diffusion length is competitive with metallic spin transport devices [23].

The above expression for $T_{\text{ff,th}}$ assumes zero magnetic field gradient for the system, but in our experiment we have a strong gradient (~ 1.3 G/nm). In the presence of a field gradient, neighbouring spins experience a field difference ΔB , and thus different Zeeman energy splittings. This can suppress flip-flops because they no longer conserve energy [24–26]. However, inhomogeneous line broadening, if on the order of ΔB , can make up this energy difference and allow flip-flops to proceed. Since the measured flip-flop time T_{ff} agrees closely to the expected zero-gradient value $T_{\text{ff,th}}$, we expect a spectral linewidth $\Delta B \gtrsim 6.5$ G.

To measure the EPR spectrum of the spin wire, we implemented a modified iOSCAR protocol which improves spatial resolution and therefore provides the capability to resolve spectral features (since spatial and spectral resolution are directly related in magnetic resonance imaging). A conventional iOSCAR measurement utilizes the entire detection volume swept out by the cantilever oscillation, as this couples to the largest number of spins and creates the largest force signal. By truncating the detection volume to the most-sensitive portion, we couple only to spins in this smaller region while maintaining high force sensitivity. Utilizing this technique (further details in SI), which we call partially-interrupted OSCAR (piOSCAR), we again scan the detection volume into the spin wire. The improved resolution enables us to resolve a staircase structure with three steps (Fig. 2c), corresponding to the three peaks of the P1 center’s hyperfine spectrum as discussed below.

The P1 centre is a substitutional nitrogen defect with an unpaired spin- $\frac{1}{2}$ electron hyperfine coupled to the spin-1 nitrogen nucleus. The hyperfine interaction results in a triplet of peaks in the EPR spectrum (Fig. 2a) corresponding to the three nuclear spin states, $m_I = -1, 0, 1$. The hyperfine splitting for our diamond crystal orientation relative to the external field is 33 G (see SI and ref. [27]). In the magnetic field gradient of our probe magnet, this splitting results in three spatially distinct spin detection volumes, with each volume defined by the contour of magnetic field which satisfies the resonance condition

for a particular hyperfine transition (Fig. 2b). We observe a step-like increase in the spin signal as each volume enters the wire and the cantilever becomes coupled to an additional hyperfine transition (Fig. 2c). The spacing between steps ($s = 25$ nm) provides an accurate means of measuring the probe field gradient, because the spacing is set by the ratio of the known hyperfine splitting (33 G) to the gradient, which we find to be $1.3 \frac{\text{G}}{\text{nm}}$. This is consistent with our estimations of gradient obtained using a standard technique [28]. The staircase structure in figure 2c is a convolution of the implanted spin density (approximately a step function), our force sensitivity profile, and the EPR spectrum of spins in the sample; deconvolution reveals the EPR spectrum shown in Fig. 2d (details in SI). From the spectrum we find an average linewidth of 7.6 G, which agrees with the expected linewidth from above, and corroborates the transport we measure in the spin wire.

In conclusion, we have measured flip-flop-mediated spin transport in an insulating diamond spin wire in the complete absence of charge transport. This transport arises from the intrinsic spin dynamics of dipole-coupled P1 centres at thermal equilibrium, which we observe by measuring spin noise without imposing a polarization gradient. By spatially resolving the three electron spin populations (corresponding to the three spin states of the hyperfine-coupled nitrogen nucleus) we obtained the EPR spectrum of less than 100 net spins in the spin wire. The resulting linewidth confirms that flip-flop mediated spin diffusion is responsible for the observed spin transport. The spectrum also enables accurate measurement of the applied magnetic field gradient. These measurements provide insight into the mechanisms of spin transport relevant for the development of nanoscale spin device elements.

Methods The ultra-soft silicon cantilever has a spring constant of 100 $\mu\text{N/m}$, resonance frequency of about 3 kHz, and approximate dimensions of 90 microns in length, 1 micron width, and 100 nm thickness. Displacement of the cantilever is measured through a 1550 nm laser interferometer. The MRFM measurements were taken at temperatures of 4.2 K. The measured moment of the SmCo_5 magnetic particle was 3.6×10^{-12} J/T. The niobium resonator coil had about 2.5 turns and a 300 micron diameter, and the resonance bowl had a diameter of about 3 microns. The diamond sample studied in this experiment had a background nitrogen concentration of 0.3 ppm ($5.27 \times 10^{16} \text{ cm}^{-3}$). To create the high spin-density wire,

the sample was first prepared using electron beam patterning and then exposed to nitrogen ion implantation at a variety of energies to create a uniform spin density. Finally the sample was annealed to yield an approximately uniform, channel (6 ppm or $1.06 \times 10^{18} \text{ cm}^{-3}$) with width, depth, and length of 200 nm , 250 nm , and 4 microns , respectively. The sample was purchased commercially from Element Six, grown via chemical vapor deposition, and the nitrogen ion implantation was performed by Leonard Kroko Inc.

Acknowledgements The research presented in this manuscript was financially supported by the Army Research Office (grant number W911NF-09-1-0147), the National Science Foundation (grant number DMR-0807093), and the Center for Emergent Materials (CEM), an NSF funded MRSEC (grant number DMR-0820414). Technical support was provided by the NanoSystems Laboratory at the Ohio State University. The authors would like to thank R. J. Furnshahl for valuable discussions related to the simulations.

References

- [1] Wolf, S. *et al.* Spintronics: A spin-based electronics vision for the future. *Science* **294**, 1488–1495 (2001).
- [2] Hanson, R., Dobrovitski, V. V., Feiguin, A. E., Gywat, O. & Awschalom, D. D. Coherent dynamics of a single spin interacting with an adjustable spin bath. *Science* **320**, 352–355 (2008). URL <http://www.sciencemag.org/content/320/5874/352.full.pdf>.
- [3] Balasubramanian, G. *et al.* Ultralong spin coherence time in isotopically engineered diamond. *Nature Materials* **8**, 383–387 (2009). URL <http://dx.doi.org/10.1038/nmat2420>.
- [4] Takahashi, S., Hanson, R., van Tol, J., Sherwin, M. S. & Awschalom, D. D. Quenching spin decoherence in diamond through spin bath polarization. *Phys. Rev. Lett.* **101**, 047601 (2008). URL <http://link.aps.org/doi/10.1103/PhysRevLett.101.047601>.
- [5] Heinrich, B. *et al.* Dynamic exchange coupling in magnetic bilayers. *Physical review letters* **90**, 187601 (2003).
- [6] Pfaff, W. *et al.* Demonstration of entanglement-by-measurement of solid-state qubits. *Nat Phys* **9**, 29–33 (2013). URL <http://dx.doi.org/10.1038/nphys2444>.
- [7] Grinolds, M. *et al.* Nanoscale magnetic imaging of a single electron spin under ambient conditions. *Nature Physics* (2013).
- [8] Mamin, H. J., Budakian, R., Chui, B. W. & Rugar, D. Detection and manipulation of statistical polarization in small spin ensembles. *Phys. Rev. Lett.* **91**, 207604 (2003). URL <http://link.aps.org/doi/10.1103/PhysRevLett.91.207604>.
- [9] Bloembergen, N. On the interaction of nuclear spins in a crystalline lattice. *Physica* **15**, 386–426 (1949).
- [10] Zhang, S., Meier, B. H. & Ernst, R. R. Polarization echoes in nmr. *Phys. Rev. Lett.* **69**, 2149–2151 (1992). URL <http://link.aps.org/doi/10.1103/PhysRevLett.69.2149>.
- [11] Lou, X. *et al.* Electrical detection of spin transport in lateral ferromagnet–semiconductor devices. *Nature Physics* **3**, 197–202 (2007).
- [12] Abragam, A. *The Principles of Nuclear Magnetism* (Clarendon, Oxford, 1961).
- [13] Vinante, A., Wijts, G., Usenko, O., Schinkelshoek, L. & Oosterkamp, T. Magnetic resonance force microscopy of paramagnetic electron spins at millikelvin temperatures. *Nature communications* **2**, 572 (2011).
- [14] Eberhardt, K. W., Mouaziz, S., Boero, G., Brugger, J. & Meier, B. H. Direct observation of nuclear spin diffusion in real space. *Physical review letters* **99**, 227603 (2007).
- [15] Fong, K. C., Herman, M. R., Banerjee, P., Pelekhov, D. V. & Hammel, P. C. Spin lifetime in small ensembles of electron spins measured by magnetic resonance force microscopy. *Phys. Rev. B* **84**, 220405 (2011). URL <http://link.aps.org/doi/10.1103/PhysRevB.84.220405>.
- [16] Muller, G. M. *et al.* Spin noise spectroscopy in gaas (110) quantum wells: Access to intrinsic spin lifetimes and equilibrium electron dynamics. *Phys. Rev.*

- Lett.* **101**, 206601 (2008). URL <http://link.aps.org/doi/10.1103/PhysRevLett.101.206601>.
- [17] Seitaridou, E., Inamdar, M. M., Phillips, R., Ghosh, K. & Dill, K. Measuring flux distributions for diffusion in the small-numbers limit. *The Journal of Physical Chemistry B* **111**, 2288–2292 (2007).
- [18] Chui, B. W. *et al.* Mass-loaded cantilevers with suppressed higher-order modes for magnetic resonance force microscopy. In *TRANSDUCERS, Solid-State Sensors, Actuators and Microsystems, 12th International Conference on, 2003*, vol. 2, 1120–1123 (IEEE, 2003).
- [19] Rugar, D., Budakian, R., Mamin, H. J. & Chui, B. W. Single spin detection by magnetic resonance force microscopy. *Nature* **430**, 329–332 (2004).
- [20] Huang, B. & Appelbaum, I. Time-of-flight spectroscopy via spin precession: The Larmor clock and anomalous spin dephasing in silicon. *Physical Review B* **82**, 241202 (2010).
- [21] Furis, M. *et al.* Local Hanle-effect studies of spin drift and diffusion in n: GaAs epilayers and spin-transport devices. *New Journal of Physics* **9**, 347 (2007).
- [22] Van Wyk, J., Reynhardt, E., High, G. & Kiflawi, I. The dependences of ESR line widths and spin-spin relaxation times of single nitrogen defects on the concentration of nitrogen defects in diamond. *Journal of Physics D: Applied Physics* **30**, 1790 (1997).
- [23] Jedema, F., Heersche, H., Filip, A., Baselmans, J. & Van Wees, B. Electrical detection of spin precession in a metallic mesoscopic spin valve. *Nature* **416**, 713–716 (2002).
- [24] Budakian, R., Mamin, H. J. & Rugar, D. Suppression of spin diffusion near a micron-size ferromagnet. *Physical Review Letters* **92**, 037205 (2004). URL <http://link.aps.org/abstract/PRL/v92/e037205>.
- [25] Genack, A. Z. & Redfield, A. G. Theory of nuclear spin diffusion in a spatially varying magnetic field. *Phys. Rev. B* **12**, 78–87 (1975). URL <http://link.aps.org/doi/10.1103/PhysRevB.12.78>.
- [26] Tyryshkin, A. M. *et al.* Electron spin coherence exceeding seconds in high-purity silicon. *Nature materials* **11**, 143–147 (2011).
- [27] Cook, R. & Whiffen, D. Electron nuclear double resonance study of a nitrogen centre in diamond. *Proceedings of the Royal Society of London. Series A. Mathematical and Physical Sciences* **295**, 99–106 (1966).
- [28] Stipe, B. *et al.* Electron spin relaxation near a micron-size ferromagnet. *Physical review letters* **87**, 277602 (2001).